Differential semblance velocity analysis via shot profile migration

*Peng Shen, Total E&P USA *, William W. Symes, Rice University, Scott Morton, Amerada Hess, and Henri Calandra, Total E&P USA*

Summary

Shot profile migration provides a convenient framework for implementation of a differential semblance algorithm for estimation of complex, strongly refracting velocity fields. The objective function minimized in this algorithm may measure either *focussing* of the image in offset or *flatness* of the image in (scattering) angle. The gradient of this objective is a by-product of a depth marching scheme, an requires a few extra computations beyond those necessary to produce the prestack data volume. A strongly refracting 2D synthetic data example illustrates the excellent image quality obtainable from model-consistent data. Offset and angle variants behave differently, with more rapid convergence for the offset variant, underlining the importance of a mathematically well posed formulation: in 2D, the angle variant is much less well-conditioned than the offset variant.

Introduction

Differential semblance velocity analysis ("DSVA", (Symes, 1986)) compares nearby image traces to refine a velocity estimate. Shen et al. (2003) presented a version of this approach to velocity estimation suitable for strongly refracting models. The algorithm described in (Shen et al., 2003) uses double-square-root ("DSR") migration to create an image volume. The failure of the migration to focus the image in (subsurface) offset is an index of velocity error. The mean square of the image volume *scaled by offset* is an objective measure of focusing failure. DSVA uses numerical minimization of this objective to update the velocity iteratively and thus minimize this objective.

Several authors have presented DSVA methods for laterally heterogeneous velocity based on other forms of migration (Symes and Versteeg, 1993; Kern and Symes, 1994; Chauris and Noble, 2001; Mulder and ten Kroode, 2002; Foss et al., 2004). Shot-geophone migration, exemplified by the DSR method, has the very significant advantage in this context of *freedom from kinematic artifacts*, which makes it especially suitable for velocity analysis in the presence of strong refraction (Stolk and Symes, 2004; Stolk et al., 2005).

This paper presents an algorithm similar to that described by Shen et al. (2003), using shot profile (rather than DSR) migration by depth extrapolation. The main computation needed in DSVA, not provided by typical implementations of shot profile migration, is the computation of the objective *gradient*. We show how the gradient may be computed by adding appropriate computations to the depth stepping loop (this is an example of the *adjoint state method*). We also compare two possible variants of the objective minimized by DSVA: the offset-domain objective, described above, and an analogous objective that measures *flatness* of image gathers parametrized by scattering angle (Sava and Fomel, 2003). We find that the straightforward measure of flatness, the angle derivative, is more difficult to optimize sucessfully than is the offset domain objective. This difficulty may be understood in terms of the mathematical properties of the two objectives. We illustrate the ability of DSVA to find an effective velocity estimate in the presence of strong lateral heterogeneity, using a 2D synthetic example based on the Marmousi velocity model (Versteeg, 1993). We create Born data using the high spatial frequencies of Marmousi as perturbation about a smoothed reference model. DSVA is able to adjust the velocity to produce a quite precise image of the reflector structure.

Differential Semblance

We will discuss explicitly the migration of 2D images, but note that much of the discussion carries over without modification to 3D migration. Image (mid)point coordinates are x and z; (migrated) offset, denoted by h, is half of the correlation distance between the downward continued source and receiver wavefields. The image volume produced by shot-geophone migration will be denoted by $I(x, z, h)$.

We restrict h to be horizontal, as is appropriate when rays carrying significant energy always make an acute angle with the vertical direction (the "DSR assumption"). We also assume that the data is *kinematically complete*, i.e. that event slownesses determine raypaths uniquely. This is the case for full 3D (areal) acquisition, also for narrow azimuth acquisition provided that crossline structural heterogeneity is mild. Under these assumptions, shot-geophone migration using a kinematically correct velocity focusses the prestack common image at the origin in offset (Stolk et al., 2005). An objective measure of focussing in offset is

$$J_h = \frac{1}{2}||P_h I||^2 = \frac{1}{2}\int h^2 I^2(x, z, h)dxdzdh. \qquad (1)$$

The differential semblance operator $P_h = h$ is a zero order differential operator, meaning that it does not change the wavenumber spectrum of I. An alternative objective function can be posed to measure the flatness of the image in angle.

$$J_\theta = \frac{1}{2}||P_\theta I||^2 = \frac{1}{2}\left||\frac{\partial}{\partial\theta}\mathscr{R}I\right|\,|^2 \qquad (2)$$

where $\mathscr{R}$ is the Radon transform (Sava and Fomel, 2003)

from offset to angle θ, $\mathscr{R}^{-1}$ its inverse. J_θ also vanishes when the velocity is kinematically correct, under the standing assumptions (Stolk et al., 2005).

Shot Profile Algorithm

Introduce source S and receiver R wavefields,

$$\begin{aligned} S(x,z,s,\omega) &= \overline{G^+(x,z,s,\omega)} \\ R(x,z,s,\omega) &= \int \overline{G^+(x,z,r,\omega)} d(r,s,\omega) dr \end{aligned}$$

which satisfy the one-way wave equations

$$\Big(\frac{\partial}{\partial z} - i\sqrt{\frac{\omega^2}{c^2}+\frac{\partial^2}{\partial x^2}}\Big) S(x,z,s,\omega) = \delta(x-s)\delta(z)$$

$$\Big(\frac{\partial}{\partial z} - i\sqrt{\frac{\omega^2}{c^2}+\frac{\partial^2}{\partial x^2}}\Big) R(x,z,s,\omega) = \delta(x-r)\delta(z) d(r,s,\omega)$$

Choose a depth step Δz, set $z_k = k\Delta z$, $k = 0,1,2,....$ Denote by $H(c^k)$ an (approximate) propagator for the operator $\left(\frac{\partial}{\partial z} - i\sqrt{\frac{\omega^2}{(c^k)^2}+\frac{\partial^2}{\partial x^2}}\right)$ from z_k to z_{k+1}, with $c^k(x) = c(x, k\Delta z)$. Setting $S^k(x,s,\omega) = S(x,k\Delta z,s,\omega)$ and similarly for R we can write the depth extrapolation scheme as

$$H(c^k)S^k = S^{k+1},\ H(c^k)R^k = R^{k+1},\ k = 0,1,2,...N_z - 1 \tag{3}$$

Initial data at the surface is $S^0(x,s,\omega) = \delta(x-s)$ and $R^0(x,s,\omega) = \int dr \delta(x-r) d(r,s,\omega)$, respectively. Here $H(c^k)$ is a linear operator on the wavefields to be extrapolated from $z = k\Delta z$ to $z = (k+1)\Delta z$. The superscript is used as the depth index for c, $c^k = c(\cdot, k\Delta z)$, and the downward continued wavefields S, R and the image in offset I as well. We write the image in offset and depth as

$$I^k(x,h) = \mathrm{Re} \sum_{s,\omega} S^k(x-h,s,\omega) R^k(x+h,s,\omega)$$

For either version of J, the gradient is

$$\nabla_c J = \left(\frac{\partial I}{\partial c}\right)^* P^* P I, \tag{4}$$

in which $P = P_h$ or $= P_\theta$. For convenience, we defined the image residual $DI = P^*PI$.

A recursive computation of the adjoint derivative $(\partial I/\partial c)^*$ is also possible; this trick is called the "adjoint state method" in the control literature, and in fact all wave equation migration methods can be viewed as instances (Stolk et al., 2005). See Shen et al. (2003) for a similar adjoint state computation for DSVA based on DSR migration.

Introduce adjoint state variables DS, DR and Dc. These fields are related to the input residual field DI by the adjoint state evolution equations

$$\begin{pmatrix} DS^{k+1} \\ DR^{k+1} \end{pmatrix} = \begin{pmatrix} H(c^k)^* DS^{k+1} + (A_S^{k+1})^* DI^{k+1} \\ H(c^k)^* DR^{k+1} + (A_R^{k+1})^* DI^{k+1} \end{pmatrix} \tag{5}$$

$$Dc^k = \left(\frac{\partial H}{\partial c^k} S^k\right)^* DS^{k+1} + \left(\frac{\partial H}{\partial c^k} R^k\right)^* DR^{k+1} \tag{6}$$

$$\begin{aligned} (A_S^k) f(x,h,s,\omega) &= f(x-h,s,\omega) R^k(x+h,s,\omega) \\ (A_R^k) f(x,h,s,\omega) &= S^k(x-h,s,\omega) f(x+h,s,\omega) \end{aligned}$$

The adjoint derivative of $H(c)S$ with respect to c must be computed, but this is generallly straightforward, as it involves only the formulae for a single step of depth extrapolation. The equations (5), (6) are to be solved in decreasing k with $DS^{N_z} = DR^{N_z} \equiv 0$, in a loop over source index and frequency. The gradient at depth level k is accumulated during this loop:

$$(\nabla_c J)^k = \mathrm{Re}\{\sum_{s,\omega} Dc^k\}.$$

Inversion

Successful optimization of the functions defined by equations (1) and (2) requires that the underlying mathematical structure of migration be respected. In particular, the velocities encountered during the iteration must remain smooth on the wavelength scale. To enforce this smoothness, we use a B-spline representation based on a relatively coarse spacing of spline nodes. Let m be a set of B-spline model parameters and B the B-spline sampling operator (onto the image grid). Restriction to velocities of the form $c = Bm$ gives a gradient in the spline parameters of the form

$$\nabla_m J(Bm) = B^* \nabla_c J(c)$$

(here $J = J_h$ or J_θ). We use a version of limited BFGS algorithm (Nocedal and Wright, 2000) to minimize J as a function of m. Only J and its gradient with respect m is needed. We have now completely described the computation of these quantities.

Examples

We constructed data consistent with the model underlying DSVA by smoothing the Marmousi model using a lowpass filter that removes any length scale smaller than 150m. The difference between the original and smoothed models served as the reflectivity γ. Synthetic Born data is expressed via the downgoing one-way Green's functions of the smoothed velocity G^+ via

$$d(r,s,\omega) = \int G^+(x,s,\omega) G^+(x,r,\omega) \gamma(x) dx,$$

and can also be computed by solving a corresponding depth extrapolation problem. The simulation is made to acquire the same number of shots as the original Marmousi dataset: the source locations span uniformly from 2.625km to 8.975km at the spacing of 0.025km. The receiver arrays are fixed for each shot and cover the entire

surface with spacing 0.01km. The migration is performed using frequencies from 3.3 to 40 Hzs on square grids of 0.01km each side. Note that use of this data in an inversion test commits an "inverse crime": the data completely agrees with the model on which the inversion is based.

Fig.1 shows the initial velocity model used in the inversion, obtained by smoothing the Marmousi model using a B-spline fitting with length scale of 2.25km by 1km (horizontal by vertical), much coarser than the resolution required for accurate imaging (see Fig.2) of the Marmousi data set (Versteeg, 1993).

Forty seven iterations of BFGS resulted in the models displayed in Figures (4) and (7). The fault block structure in the middle region has emerged in both cases; the difference appear to be subtle. The image from offset domain DSVA (Figure (3)) is a very accurate rendition of the structure of the actual Marmousi model, in all important respects. The angle domain image (Figure (6)) is of distinctly lower quality. Comparison of angle gathers (Figures (5), (8)) leads to the same conclusion: offset domain DSVA appears to have been more successful, given the expended amount of computational effort. Note that the angle gather displayed in Figure (5) is a postprocess result.

The reason for this difference in performance lies in the numerical condition of the Hessian operator. The operator P_θ is of order 1/2 (in 2D!), meaning that it scales Fourier components by the square root of frequency. The operator P_h, on the other hand, is bounded, i.e. does not enhance high frequency components. As a result, the Hessian (second derivative) operator of J_h is better conditioned than the Hessian of J_θ (finite vs. infinite condition). Convergence for Newton-like methods is heavily influenced by Hessian condition (Nocedal and Wright, 2000).

Conclusion

Both offset and angle domain versions of DSVA are effective in updating a complex velocity model involving strong refraction, though the offset domain variant as presented here is somewhat more computationally efficient. Either supplementing the operator P_θ with a negative order factor, for 2D, or computing in 3D where P_θ is bounded, would likely remove the comparative advantage of the offset domain computation.

The test demonstrated here used "perfect" data, that is, data corresponding precisely to the theory underlying DSVA. Many open questions remain concerning the sensitivity of the approach to data imperfections, on the one hand, and the possibility of similar approaches based on more sophisticated modeling, on the other.

Acknowledgement

The work of WWS was partly supported by The Rice Inversion Project.

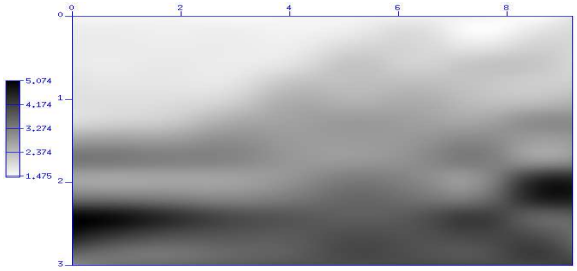

Fig. 1: Initial velocity model.

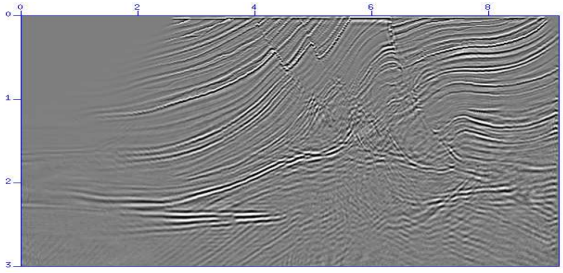

Fig. 2: Image obtained at the initial velocity model.

References

Chauris, H., and Noble, M., 2001, Two-dimensional velocity macro model estimation from seismic reflection data by local differential semblance optimization: applications synthetic and real data sets: Geophys. J. Int., **144**, 14–26.

Foss, S.-K., Ursin, B., and de Hoop, M. V., 2004, Depth-consistent P- and S-wave velocity reflection tomography using PP and PS seismic data: Expanded Abstracts,Society of Exploration Geophysicists, 53rd Annual International Meeting, 2363–2367.

Kern, M., and Symes, W., 1994, Inversion of reflection seismograms by differential semblance analysis: Algorithm structure and synthetic examples: Geophysical Prospecting, **99**, 565–614.

Mulder, W., and ten Kroode, A., 2002, Automatic velocity analysis by differential semblance optimization: Geophysics, **67**, 1184–1191.

Nocedal, J., and Wright, S., 2000, Numerical optimization: Springer Verlag, New York.

Sava, P., and Fomel, S., 2003, Angle domain common-image gathers by wavefield continuation methods: Geophysics, **68**, 1065–1074.

Shen, P., Stolk, C., and Symes, W., 2003, Automatic velocity analysis by differential semblance optimization: Expanded Abstracts, Society of Exploration Geophysicists, 73nd Annual International Meeting, 2132–2135.

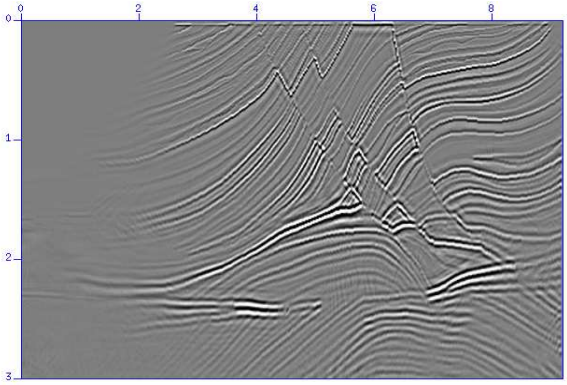

Fig. 3: Optimized image by offset domain DSO.

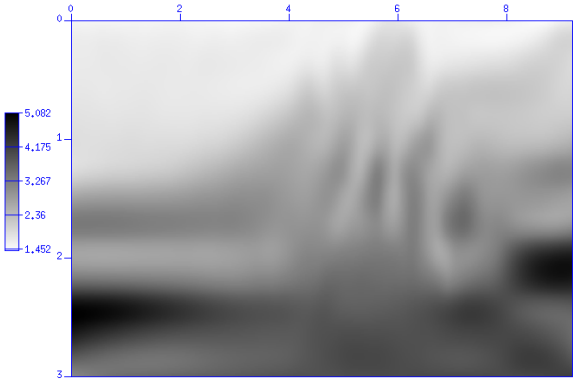

Fig. 4: Optimized velocity by offset domain DSO.

Stolk, C. C., and Symes, W. W., 2003, Smooth objective functionals for seismic velocity inversion: Inverse Problems, **19**, 73–89.

Stolk, C., and Symes, W., 2004, Kinematic aritifacts in prestack depth migration: Geophysics, **69**, 562–575.

Stolk, C. C., de Hoop, M. V., and Symes, W. W., Kinematics of shot-geophone migration:, Technical Report 05-04, Department of Computational and Applied Mathematics, Rice University, Houston, Texas, USA, 2005.

Symes, W., and Versteeg, R., 1993, Velocity model determination using differential semblance optimization: Expanded Abstracts, Society of Exploration Geophysicists, 63nd Annual International Meeting, 696–699.

Symes, W., 1986, Stability and instability results for inverse problems in several-dimensional wave propagation *in* Glowinski, R., and Lions, J., Eds., Proc. 7th International Conference on Computing Methods in Applied Science and Engineering:: North-Holland.

Versteeg, R. J., 1993, Sensitivity of prestack depth migration to the velocity model: Geophysics, **58**, 873–882.

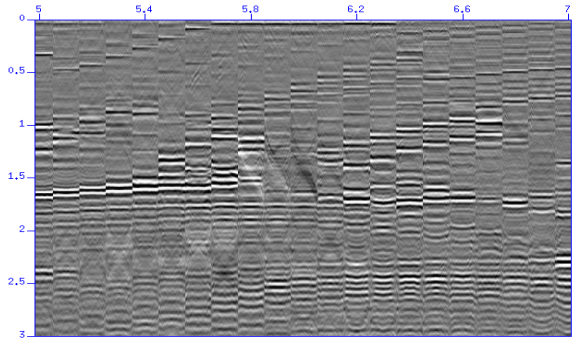

Fig. 5: The optimized angle gathers by offset domain DSO.

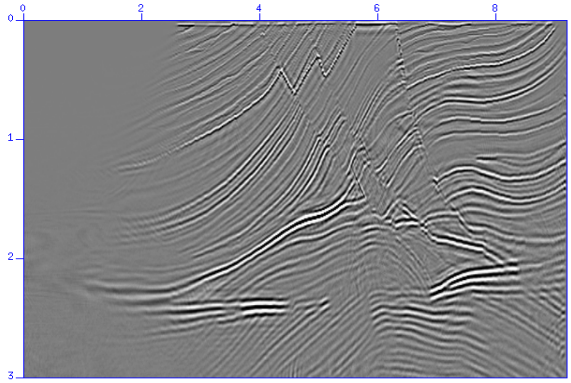

Fig. 6: The optimized image by angle domain DSO.

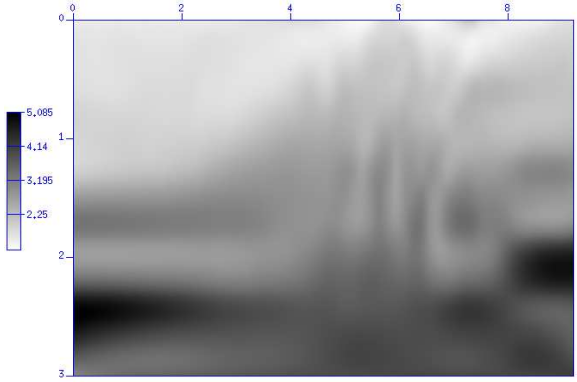

Fig. 7: The optimized velocity by angle domain DSO.

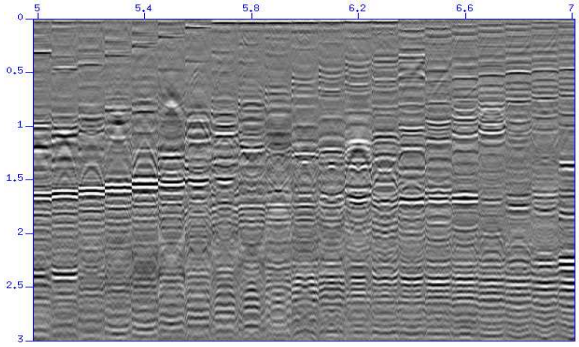

Fig. 8: The optimized angle gathers by angle domain DSO.